A classroom demonstration of reciprocal space

Morten Hannibal Madsen, Louise Høpfner, Nina Rasmussen, Mikkel Stolborg, Jesper Nygård et al.

Citation: Am. J. Phys. **81**, 274 (2013); doi: 10.1119/1.4773979
View online: http://dx.doi.org/10.1119/1.4773979
View Table of Contents: http://ajp.aapt.org/resource/1/AJPIAS/v81/i4
Published by the American Association of Physics Teachers

A classroom demonstration of reciprocal space

Morten Hannibal Madsen,[a)] Louise Høpfner, Nina Rasmussen, Mikkel Stolborg,
Jesper Nygård, Robert Feidenhans'l, and Jan W. Thomsen
Nano-Science Center, Niels Bohr Institute, University of Copenhagen, 2100 Copenhagen, Denmark

(Received 20 April 2012; accepted 17 December 2012)

An array of nanowires and a laser pointer are used for a simple visualization of two-dimensional reciprocal space. The experiment can be performed without any preparation and in any classroom. It aids the teaching of scattering experiments, and illustrates the underlying principles of electron, x-ray, and neutron scattering. A detailed study of the diffraction pattern was performed by mounting the sample with nanowires on a stage designed for x-ray scattering. The setup is well suited for undergraduate students, who get training in sample alignment in a small lab instead of at a large-scale facility. The exact positions of the diffraction spots are calculated and monitored experimentally for a 360° rotation of the sample. By fitting to this set of images, it is possible to determine the lattice vectors of the artificial crystal with an uncertainty of less than 1%. © *2013 American Association of Physics Teachers.*

[http://dx.doi.org/10.1119/1.4773979]

I. INTRODUCTION

Scientists use scattering experiments to analyze materials, with the most common sources being electron,[1] x-ray,[2,3] and neutron[4] beams. All of these techniques take advantage of the wave properties of the particles.

Typically one selects the wavelength of the incoming waves such that it matches the structure of interest. In this experiment, we do the reverse—we use a laser as the monochromatic wave source and customize an array of nanowires to fulfill the diffraction conditions. By proper design of the nanowire array, the ratio of the nanowire pitch to the laser wavelength ($\sim 3\,\mu\text{m}/0.532\,\mu\text{m} \simeq 6$) is directly comparable to the ratio of a typical crystal lattice spacing to synchrotron-generated x-rays ($\sim 3\,\text{Å}/0.5\,\text{Å} \simeq 6$).

The concept of reciprocal space is often difficult for students to comprehend.[5–7] It can be compared to learning to ride a bicycle—once you can do it, it is hard to say what is so difficult about it. The demonstration experiment described here has been used in the course "Introduction to X-Ray Physics" at the Niels Bohr Institute, and helps students better understand the subject.

Inexpensive diffraction gratings, or even a compact disk, can be used to demonstrate diffraction by a one-dimensional structure. However, gratings do not show that the points in an array can be regarded as planes, and therefore also lack the possibility of changing the diffraction pattern by rotation.

Only a few experiments for visible light interacting with nanowires have so far been reported.[8–10] None, to our knowledge, use a two-dimensional (2D) grid. In this paper, we calculate and measure the positions of the diffraction spots from a 2D array of nanowires.

II. DEMONSTRATION EXPERIMENT

A laser pointer with a wavelength in the visible band and a periodic array of nanowires are the only equipment needed for the diffraction experiment. The laser beam is pointed towards an area with precisely positioned nanowires, and the diffraction pattern is displayed directly on a white screen. The experiment can be performed without any preparation and works every time. The only thing to be aware of is stray laser light, as this may cause eye damage. With proper handling and a low power laser (1 mW), classroom experiments are safe.

The sample can be held in one hand and the laser pointer in the other, and by rotating the sample, one can watch the diffraction spots appear and disappear. In Fig. 1(a), a simple mount is used for the laser and the sample. Different arrays of positioned nanowires give easily distinguishable diffraction patterns. Likewise, different colored laser pointers (e.g., red, green, and blue) can be used to illustrate the wavelength dependence of the diffraction conditions.

A. Entering reciprocal space

Diffraction arises from interference of electromagnetic waves (e.g., visible light or x-rays) when scattered on planes. Scattering on an array of points (e.g., nanowire arrays or atoms in a crystal lattice) can be regarded as scattering on planes, as shown in Fig. 1(e), and is described by Bragg's law,

$$2d \sin\theta = n\lambda, \tag{1}$$

where λ is the wavelength of the incoming wave, n is an integer, d is the lattice spacing, and θ is the angle between the incoming wave and the scattering planes. From Eq. (1), it is seen that Bragg's law is satisfied only for $\lambda \leq 2d$.

One can also use the Laue condition,[6]

$$\Delta\vec{k} = \vec{G}, \tag{2}$$

to describe scattering from planes using a vector formalism. Here the scattering vector $\Delta\vec{k} = \vec{k}' - \vec{k}$ is defined as the difference between the diffracted and incoming wavevectors, and $\vec{G}$ is a reciprocal lattice vector given by

$$\vec{G} = h\vec{b_1} + k\vec{b_2} + l\vec{b_3}, \tag{3}$$

where $\vec{b_1}$, $\vec{b_2}$, and $\vec{b_3}$ are unit vectors of the reciprocal space, and h, k, and l are integers known as Miller indices.[11]

For an interpretation of the Laue condition, one can look at an algebraic statement of the scattering wave vector, as in Ref. 6. For elastic scattering, where no energy is transferred to the crystal, the magnitude of the scattering wave vector can be written as

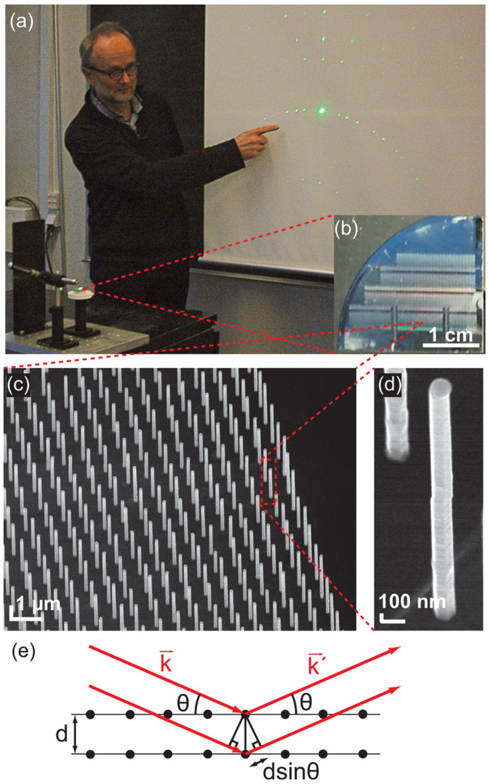

Fig. 1. Optical light scattering on a periodic array of nanowires. (a) Classroom setup of the experiment to illustrate reciprocal space. (b) Optical image of a substrate with different densities of nanowires. (c and d) SEM images of InAs nanowires positioned using e-beam lithography. The image is taken from a 15° angle, and the height is given by the vertical scalebar. (e) Sketch of Bragg's law. When $2d\sin\theta$ equals an integer number of wavelengths $n\lambda$, constructive interference leads to a diffraction spot.

$$|\Delta\vec{k}| = 2|\vec{k}|\sin\theta. \tag{4}$$

By substituting the Bragg condition $2d\sin\theta = \lambda$ and $|\vec{k}| = 2\pi/\lambda$ into Eq. (4), one obtains $|\Delta\vec{k}| = 2\pi/d$. It is seen that the scattering wave vector in reciprocal space is a representation of real space parameters with a characteristic scaling factor of 2π. One should note that the typical length scale in reciprocal space is 2π over the typical scale in real space.

B. The Ewald circle

The diffraction pattern in three dimensions can be represented using a geometrical construction called the Ewald sphere. Here, we consider the 2D case and hence the Ewald circle, as sketched in Fig. 2.

The Ewald circle is constructed by considering the reciprocal lattice of a crystal with origin O. The incident wave vector $\vec{k}$ is drawn, such that it ends at O. Now a circle that passes through O and with radius $|\vec{k}|$ is drawn. The angle between the two vectors is 2θ, as we assume that the scattering is elastic. Any other point of the reciprocal lattice that the circle intersects fulfills the Laue condition ($\Delta\vec{k} = \vec{G}$), and will therefore give rise to a diffraction spot.

The length of the incoming wave vector is inversely proportional to the wavelength of the wave, $|\vec{k}| = 2\pi/\lambda$. If the wavelength is decreased, the radius of the Ewald circle increases, and more diffraction spots will be visible. This can be demonstrated by using different colored laser pointers.

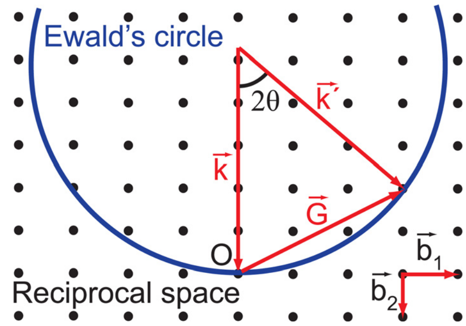

Fig. 2. Ewald construction in the 2D case. The incident wave vector $\vec{k}$ defines the radius of the Ewald circle, and the elastic outgoing wave vectors $\vec{k}'$ are given for all spots were Bragg's condition is fulfilled.

C. Fabrication of ordered arrays of nanostructures

Areas with ordered arrays of nanostructures can be fabricated using photo- or electron-beam lithography. Electron-beam lithography has the highest resolution but is a slow process, where one point has to be written at a time, whereas photolithography can process a full wafer at a time. Photolithography is especially used in the semiconductor industry; for instance, a modern microprocessor chip is fabricated using several steps of lithography. The diffraction experiment described in this paper works well with samples fabricated by UV lithography. For example, nickel pillars with a pitch of 10 μm, a diameter of 1.5 μm, and a height of 600 nm have been found to give a clear diffraction pattern. A guide for fabrication of such ordered arrays using standard lithography techniques can be found in the online supplement.[12]

For this study, we have used nanowires positioned by electron-beam lithography.[13] Nanowires are best described as elongated crystals. They are fabricated using a molecular beam epitaxy (MBE) system and a more detailed description of nanowire growth in the same system can be found in Ref. 14.

Structures with a variety of densities and patterns were fabricated, with pitches in the range 2–10 μm and in quadratic, rectangular, and hexagonal grids. We choose a 4 μm $\times$ 3 μm rectangular grid, with nanowires 1 μm long and 100 nm wide for the in-depth analysis.

III. EXPERIMENT FOR STUDENTS

The diffraction experiment is good for undergraduate students; it takes only minutes to set up but there are unlimited options to fine-tune it. The setup provides challenges for students at all levels and therefore the experiment meets some of the most important requirements for a good project: easy setup, fast acquisition of data, and unlimited improvements. Furthermore, the experiment is valuable training in sample alignment for students who are interested in scattering experiments at large-scale facilities (e.g., neutron or x-ray sources) as the procedures are similar.

A. Calculation of the diffraction pattern

The exact positions of the diffraction spots can be calculated using the Laue condition, Eq. (2), and the geometric interpretations of the total system. A sketch of the diffraction setup for the experiments is shown in Fig. 3, where all quantities are geometrically defined. Monochromatic light is coming in from the left, represented by the incoming wave vector $\vec{k}$. In our case it is a laser source, but it could in principle be

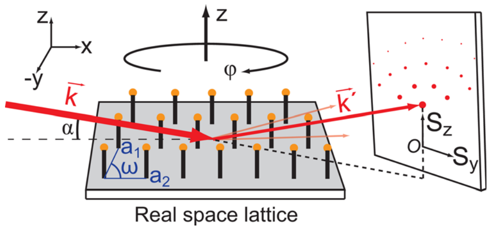

Fig. 3. Schematic diagram of the scattering experiment. Monochromatic light comes in from the left, scatters on nanowires positioned in an array, and produces diffraction spots to the right.

any monochromatic waves, such as synchrotron-generated x-rays when the lattice spacing is on the atomic scale. The incoming light scatters on the nanowires, which are positioned in a 2D array spanned by the real plane lattice vectors $\vec{a}_1$ and $\vec{a}_2$. For the derivation presented here, we will assume that the lattice vectors are orthogonal (i.e. $\omega = 90°$). The diffracted beams that fulfill the Bragg conditions will give rise to diffraction spots observed on a screen a distance L from the crystal. The positions of diffraction spots are calculated as a horizontal S_y and a vertical S_z distance from the origin on the screen. The origin is set to be right between the 0th order diffraction spot, also called the specular spot, and a not-visible spot from a beam passing directly through the sample without any reflection or scattering, as indicated in Fig. 3.

The components of the incoming wave vectors can be found by geometrical considerations, and are in the (x, y, z) system given by

$$\vec{k} = \frac{2\pi}{\lambda}\begin{pmatrix} \cos\alpha \\ 0 \\ -\sin\alpha \end{pmatrix}, \tag{5}$$

where α denotes the angle between $\vec{k}$ and the plane of incidence. The real plane primitive vectors are rotated by the angle ϕ around the z-axis with respect to the incoming wave vector. In the (x, y) coordinate system, they are therefore given by

$$\vec{a}_1 = d_1\begin{pmatrix} \cos\phi \\ \sin\phi \\ 0 \end{pmatrix} \tag{6}$$

and

$$\vec{a}_2 = d_2\begin{pmatrix} -\sin\phi \\ \cos\phi \\ 0 \end{pmatrix}, \tag{7}$$

where d_1 and d_2 are the real space lattice spacings. The simplest vector perpendicular to both $\vec{a}_1$ and $\vec{a}_2$ is

$$\vec{n} = \begin{pmatrix} 0 \\ 0 \\ 1 \end{pmatrix}. \tag{8}$$

For the reciprocal lattice vector $\vec{G}$, one first needs to find the primitive reciprocal lattice vectors. These are found through[11]

$$\vec{b}_1 = 2\pi\frac{\vec{a}_2 \times \vec{n}}{\vec{a}_1 \cdot \vec{a}_2 \times \vec{n}} \tag{9}$$

and

$$\vec{b}_2 = 2\pi\frac{\vec{n} \times \vec{a}_1}{\vec{a}_1 \cdot \vec{a}_2 \times \vec{n}}, \tag{10}$$

resulting in

$$\vec{G} = h\vec{b}_1 + k\vec{b}_2 = 2\pi \cdot \begin{pmatrix} \frac{h}{d_1}\cos\phi - \frac{k}{d_2}\sin\phi \\ \frac{h}{d_1}\sin\phi + \frac{k}{d_2}\cos\phi \\ 0 \end{pmatrix} \tag{11}$$

for scattering on a 2D crystal.

The horizontal and vertical distances from the origin to the (hk) diffraction spot are denoted S_y and S_z, respectively, and also indicated in Fig. 3. The ratio of S_y to the screen distance L is equal to the ratio of the y-component of the diffracted wave vector to its x-component; that is,

$$\frac{S_y}{L} = \frac{k'_y}{k'_x}. \tag{12}$$

By substituting Eqs. (5) and (11) into the Laue condition (2), an expression for k'_y and k'_x is found, which, when combined with Eq. (12), gives

$$S_y = L \cdot \frac{(h/d_1)\sin\phi + (k/d_2)\cos\phi}{(1/\lambda)\cos\alpha + (h/d_1)\cos\phi - (k/d_2)\sin\phi}. \tag{13}$$

In a similar way, the vertical deflection can be calculated, although k'_z is slightly more cumbersome to calculate. Here, we use the fact that the length of the diffracted wave vector can be written as

$$|\vec{k}'|^2 = k'^2_x + k'^2_y + k'^2_z. \tag{14}$$

Using the Laue condition (2), this is equivalent to

$$k'^2_z = |\vec{k}'|^2 - (k_x + G_x)^2 - (k_y + G_y)^2. \tag{15}$$

As we assume elastic scattering, the length of the scattered wave vector is equal to the incoming one, that is, $|\vec{k}|^2 = |\vec{k}'|^2 = (2\pi/\lambda)^2$. Substituting Eqs. (5) and (11) into Eq. (15) then gives

$$k'^2_z = 4\pi^2\left[\frac{1}{\lambda^2}(1 - \cos^2\alpha) - \frac{h^2}{d_1^2} - \frac{k^2}{d_2^2} + \frac{2\cos\alpha}{\lambda}\left(\frac{k}{d_2}\sin\phi - \frac{h}{d_1}\cos\phi\right)\right]. \tag{16}$$

Finally, the vertical deflection on the screen is found to be

$$S_z = L \cdot \frac{k'_z}{(1/\lambda)\cos\alpha + (h/d_1)\cos\phi - (k/d_2)\sin\phi}. \tag{17}$$

The above calculations have assumed a rectangular grid for the crystal structure. For $\omega \neq 90°$, the basis lattice vectors must be modified accordingly. In the case of $\omega > 90°$, Eqs. (6) and (7) are modified to

$$\vec{a}_1 = d_1 \begin{pmatrix} \cos\phi \\ \sin\phi \\ 0 \end{pmatrix} \tag{18}$$

and

$$\vec{a}_2 = d_2 \begin{pmatrix} -\sin\phi \sin\omega + \cos\omega \cos\phi \\ \cos\phi \cos\omega + \cos\phi \sin\omega \\ 0 \end{pmatrix}. \tag{19}$$

By repeating the calculations above, one can derive the modified versions of Eqs. (13) and (17) to account for a non-rectangular lattice.

B. Experimental setup

Though a minimalistic setup is sufficient for understanding the basic principles, a more advanced setup is needed to take full advantage of the derived theory (see Fig. 4). The sample is mounted on a two-axis goniometer on top of a 360° turntable [Fig. 4(b)]. The two axes of freedom from the goniometer can be used to center the sample, such that it rotates around the same point, when the turntable is rotated. This mimics the setup of a standard x-ray diffraction experiment with 3 S + 2D degrees of freedom, meaning that three circle motions can control the sample, and two circle motions the detector. The setup is such that the angle of incidence is equal to the detector angle. The whole setup is mounted on a bread board for optimal stabilization.

A HeNe laser with a wavelength of $\lambda = 632.8$ nm is used as the coherent light source. This type of laser has the advantage of a low output intensity, and some models are equipped with a range of neutral density filters, making it possible to have an output intensity of less than 1 mW; HeNe lasers are therefore very suitable for student experiments. Three lenses, with focal lengths of 100 cm, 12.5 cm, and 5 cm are used in the setup as illustrated in Fig. 4(c). The first lens is used to obtain a collimated beam and the two others are set in a telescope configuration to decrease the beam size by a factor of 0.4.

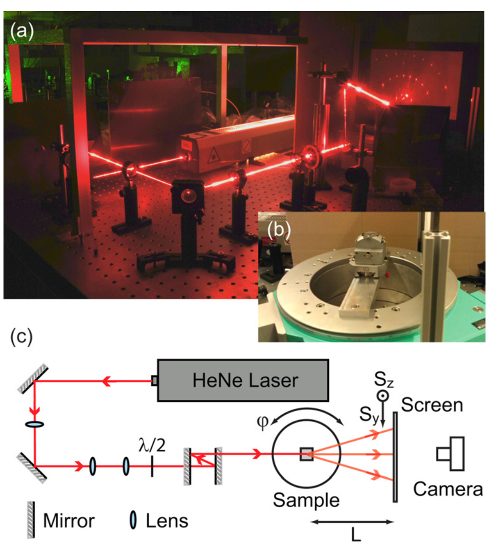

Fig. 4. Experimental setup. (a) Image showing the full setup and the alignment of the laser on the sample and the diffraction pattern. (b) Sample mounted on a two-axis goniometer on top of a 360° turntable. (c) A schematic diagram of the setup. The first lens is used to obtain a collimated beam and the two others are set in a telescope configuration to decrease the beam size by a factor of 0.4. The two mirrors next to the sample are for elevating the beam and pointing it down at the sample with an angle $\alpha = 15.6°$, close to Brewster's angle for InAs.

Mirrors with micrometer screws are used for guiding the beam. The two mirrors closest to the sample are used to raise the beam and point it down at the center of the sample. The angle of incidence can be varied by moving these mirrors.

The amount of unwanted scattering can be reduced greatly by taking advantage of Brewster's angle.[15] At an angle determined by the indices of refraction for the media, only light polarized perpendicular to the plane of incidence is reflected. By using a half-wave plate ($\lambda/2$) to linearly polarize the beam parallel to the plane of incidence, most of these reflections can be eliminated. For InAs, Brewster's angle is $\theta_B = 73.8°$ with respect to the plane of incidence, and therefore an incidence angle close to $\alpha = 90° - \theta_B = 16.2°$ is used in the setup. We found this step of major importance, as the background was reduced by a factor of five. Reducing the room light gives additional signal-to-noise improvement.

A white sheet of paper was used for the screen, as it had a good thickness and texture. Various other types of materials were tested for the screen, but none could beat the white paper. Furthermore, the paper had the advantage of being straightforward to print a grid on for scaling.

For data acquisition, a Nikon D40 digital single-lens reflex camera is used; it has a charged-coupled-device (CCD) sensor with a 6.1 megapixel resolution. Data are saved in RAW format ensuring no loss of quality due to compression. The camera was first checked for dead pixels by taking a picture with the camera lens covered, loading it into MATLAB, and looking for pixels with a zero intensity value. Two dead pixels were found and these were omitted in later data analysis. All images are acquired in full manual mode with an aperture of 1/4.0 and a shutter time of 1/3 s.

C. Analysis of a single image

For a given setup, an image is acquired with the digital camera and transferred to a computer. MATLAB is used for the manipulation and measurements of the images.

A 3D plot of the data before background subtraction is shown in Fig. 5(a), where the intensity is plotted along the z-axis. Because a lot of noise is present, even for an image obtained in a dark room at Brewster's angle, the data are filtered. First, a background image is made using morphological opening of the image by removing all disk-shaped spots in the image with a radius less than 24 pixels.[16] This background image is then subtracted from the original image. Second, a threshold value is defined, high enough to remove random noise pixels but low enough to include the peaks. A binary image is now formed and used as a mask on the original image, thereby creating an image with only nonzero values at the peak positions. The final result is shown in Fig. 5(b). A more intuitive way of subtracting the background is to use ImageJ,[17] where a threshold value can be chosen graphically, and the "analyze particle" function set to count areas only in a certain size range.

Based on the theoretical framework derived in Sec. III A, the diffraction spots on the obtained images can be categorized; an example is shown in Fig. 5(c). A script written in MATLAB calculates the theoretical position of the peaks using the modified version of Eqs. (13) and (17), and looks for the experimental intensity peak in the vicinity of this spot. The

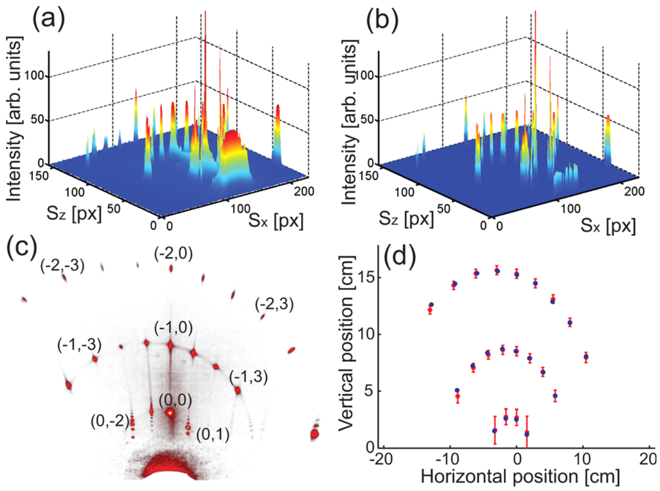

Fig. 5. Measurement on a rectangular grid of nanowires. (a) Raw data. (b) Data with background subtracted. (c) Diffraction spots on the screen. (d) Experimental [red (light gray) dots with errorbars] and theoretically calculated [blue (dark gray) dots without errorbars] diffraction spots.

calculated and experimental intensity peaks are plotted in Fig. 5(d). It is clear that the diffraction pattern is a mapping of the reciprocal lattice. All expected spots are visible and can be labeled using this algorithm.

Some of the lower-order diffraction spots are degenerate. This is due to a secondary periodicity with larger lattice distance, introduced by the stitching during the e-beam lithography. For this study we look only at the brightest spot, which is expected to be the 0th-order diffraction from the secondary lattice.

In Fig. 5(d), both the theoretically derived and experimentally found positions of the diffraction spots are plotted. The uncertainties in the theoretical values come from the measured angles and distances in the nanowire arrays. The values used in this study are summarized in Table I along with their estimated uncertainties.

D. Aligning the sample for rotation

The diffraction pattern changes when the sample is rotated around ϕ. This change can be used to calculate the lattice structure by fitting peaks for different angles. For instance, d_1, d_2, and ω can be estimated in this way. To test the setup, a group of students was given a sample with $\omega = 95^\circ$ but told that it was a rectangular lattice. Using the method described below, they detected this deception and were able to estimate ω within 0.2°.

The basic protocol to align a sample for a scattering experiment is:

1. Decide on the basic parameters, including wavelength and scattering configuration.
2. Find the center of the sample, or the point of interest.
3. Adjust the sample to rotate uniformly around the point where the incoming beam hits the sample.
4. Align the system parameters to the reciprocal lattice vectors of the crystal.

The basic parameters are determined by the laser system and the requirement for fulfilling the Brewster's angle condition. The second step is relatively straightforward as the HeNe laser emits light in the visible range. The rough alignment is made by hand and subsequently fine-tuned using the micrometer screws on the mounts of mirrors 3 and 4.

The next step is more challenging and required the use of the two-axis goniometer. The turntable is rotated (angle ϕ) while monitoring the specular intensity peak. The goniometers are now adjusted until the specular intensity peak remains stationary during a 360° rotation. Measurements of the aligned sample are shown in Fig. 6(a); the position deviates by less than 0.5 mm throughout a full rotation of the sample.

The last step is performed by rotating the sample until the intensity peaks for (0, 0), (–1, 0), and (–2, 0) are vertically aligned, and (0, -1) and (0, 1) horizontally aligned, defined as $\phi = 0^\circ$. For a rectangular lattice, a rotation of $\phi = 90^\circ$ should bring the system into another configuration where the spanned planes are perpendicular. The lack of this symmetry led the students to discover the skewed lattice.

When identifying the diffraction points a systematic deviation of the experimental position was found. The deviation was found to increase with the distance to the specular spot, which can be attributed to the screen being slightly tilted, an imperfect lattice, and/or lens distortions. The camera lens was investigated for distortion effects (e.g., spherical aberration and coma) by imaging a piece of paper with a printed millimeter scale, and found to be negligible for the given setup (<1 mm). Given that the screen has been properly aligned (i.e., not tilted), the deviation from this effect should be small as well. The main deviation therefore originates from an imperfect lattice. To correct for this, we gathered

Table I. Experimental parameters. These values are used throughout the experiment unless otherwise stated.

Quantity	Value	Std. dev.
d_1	2.90 μm	$\pm$0.05 μm
d_2	3.90 μm	$\pm$0.05 μm
L	9.4 cm	$\pm$0.1 cm
ϕ	Varies	$\pm0.1^\circ$
α	15.6	$\pm0.1^\circ$

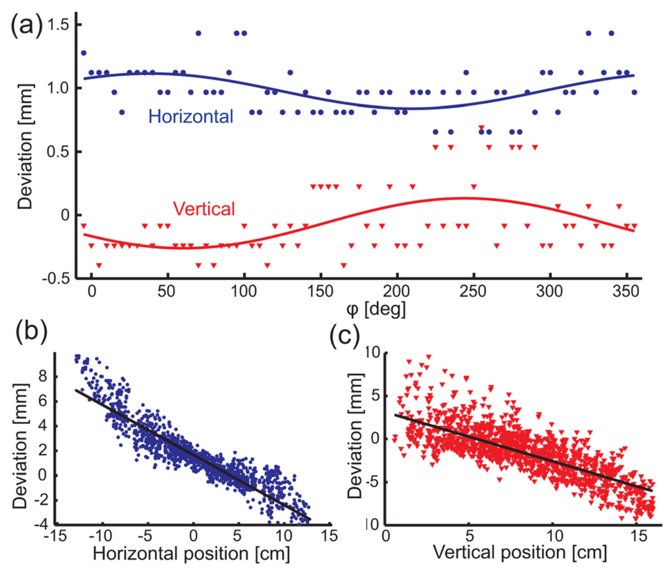

Fig. 6. Deviations of the diffraction points. (a) The movement of the specular spot when the sample is rotated. It can be seen that the sample is very well aligned in both the horizontal and vertical directions. (b) Vertical and (c) horizontal deviations of the experimentally observed diffraction spots from the theoretically derived values.

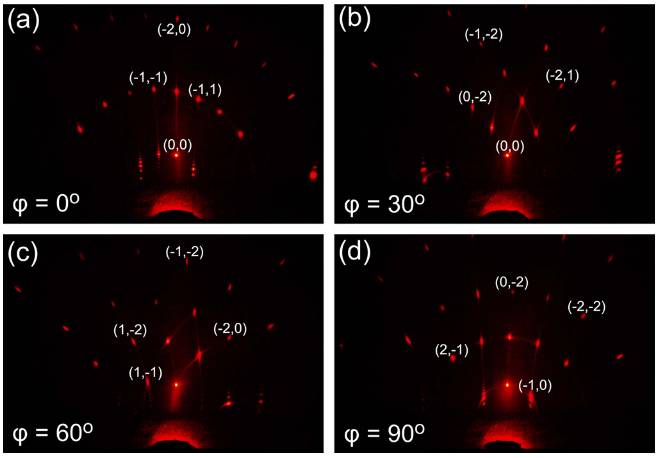

Fig. 7. Images of the diffraction patterns for different rotation angles ϕ of the sample. The alignment of the sample is optimized such that the position of the specular spot (0, 0) is static under rotation. See the online article for a video made from a collection of images showing a full rotation at 5° intervals. The video is also available as supplementary material (see Ref. 12) (enhanced online) [URL: http://dx.doi.org/10.1119/1.4773979.1].

the deviation from the theoretically calculated position of every diffraction spot for *all* the data points. Plots of the vertical and horizontal deviations are shown in Figs. 6(b) and 6(c), respectively. To adjust for all of the above described effects, a linear fit was made to all the data points and this was subtracted from the measurements.

E. Advanced experiments

The sample is rotated around ϕ and images acquired with an interval of 5° for a full rotation of 360°. A few of the images are shown in Fig. 7 and all the images have been collected into a movie. It is noteworthy that the position of the specular peak (0, 0) is almost stationary during the rotation, showing that the sample has been properly aligned. The images are analyzed using the software described in Sec. III C, and the values d_1, d_2, and ω are derived. The calculated values have a deviation of less than one percent from the data obtained using a scanning electron microscope (SEM). However, SEM length measurements are not exact because they depend on how well the beam is focused on the sample. The SEM images were analyzed using the software ImageJ.[17]

The setup can be further improved to obtain additional results. For instance, one could use a 2D detector, instead of the white paper, to improve the sensitivity. In this case, it might be possible to measure the intensity of the individual points precisely enough to calculate the form factor, and thereby obtain the height and width of the nanowires.

A more advanced experiment would be to calculate the Young's modulus of the nanowires. This can, for instance, be done by monitoring the intensity of a single diffraction spot and noting how this changes when the nanowires are set to vibrate.

In addition, using a small laser beam and a system for scanning the surface of the crystal, e.g., by mounting piezos on the backside of the mirrors, one could potentially check an array of nanowires for defects. Such a procedure would be valuable in large-scale production of vertical transistors, as one defect could render the device useless.

IV. CONCLUSION

With a periodic array of nanowires and a laser, we have mimicked the diffraction conditions for a crystal in a synchrotron beam. This experiment can be used as a simple classroom demonstration of reciprocal space and as an individual undergraduate experiment. For teaching, this experiment has already proven to be a valuable tool for easier understanding of reciprocal space, and to see the connection to x-ray-, neutron-, and electron-scattering experiments.

As an experiment for students this exercise fulfills several important requirements. Most importantly, it is relatively easy to obtain the initial results; it is also possible to improve the setup and the range of experiments is limited only by your imagination. By comparing the theoretically derived positions of the diffraction spots to the experimental results for a variety of different angles, the structure factor of the artificial crystal has been determined with an accuracy of less than 1%.

ACKNOWLEDGMENTS

The authors would like to thank Anastasiya A. Lavell, Andrew Higginbotham, and Erik Johnson for careful proofreading. The authors acknowledge support for e-beam lithography from UNIK Synthetic Biology, and MBE growth from the Danish Strategic Research Council.

[a]Electronic mail: Hannibal@nbi.dk

[1]D. B. Williams and C. B. Carter, *Transmission Electron Microscopy*, 2nd ed. (Springer, New York, 2009).
[2]J. Als-Nielsen and D. McMorrow, *Elements of Modern X-ray Physics*, 2nd ed. (John Wiley & Sons, West Sussex, England, 2010).
[3]B. D. Cullity, "One- and two-dimensional x-ray diffraction," Am. J. Phys. **19**(9), 500–506 (1951).
[4]G. L. Squires, *Introduction to the Theory of Thermal Neutron Scattering* (Dover, Mineola, NY, 1996).
[5]R. L. Liboff, "Display of real-space scattering in the Ewald construction," Am. J. Phys. **60**(12), 1152 (1992).
[6]L. E. Radford, "Equal rights for the reciprocal lattice," Am. J. Phys. **43**(8), 697–700 (1975).
[7]R. T. Bush, "The Ewald construction and the Bragg law of diffraction in a first course in solid-state physics," Am. J. Phys. **37**(6), 669 (1969).
[8]M. Lexholm, D. Hessman, and L. Samuelson, "Optical Interference from pairs and arrays of nanowires," Nano Lett. **6**, 862–865 (2006).
[9]M. Lexholm, I. Karlsson, F. Boxberg, and D. Hessman, "Optical determination of Young's modulus of InAs nanowires," Appl. Phys. Lett. **95**, 113103 (2009).
[10]S. O. Mariager, D. Khakhulin, H. T. Lemke, K. S. Kjær, L. Guerin, L. Nuccio, C. B. Sørensen, M. M. Nielsen, and R. Feidenhans'l, "Direct observation of acoustic oscillations in InAs nanowires," Nano Lett. **10**(7), 2461–2465 (2010).
[11]C. Kittel, *Introduction to Solid State Physics* (John Wiley & Sons, New York, 2004).
[12]See supplementary material at http://dx.doi.org/10.1119/1.4773979 for a guide on fabrication of ordered arrays and a video of diffraction images showing a full rotation of an array with nanowires.
[13]T. Mårtensson, M. Borgström, W. Seifert, B. J. Ohlsson, and L. Samuelson, "Fabrication of individually seeded nanowire arrays by vapour liquid solid growth," Nanotechnology **14**, 1255–1258 (2003).
[14]M. H. Madsen, P. Krogstrup, E. Johnson, S. Venkatesan, E. Mühlbauer, C. Scheu, C. B. Sørensen, and J. Nygård, "Experimental Determination of Adatom Diffusion Lengths for Growth of InAs Nanowires," J. Cryst. Growth (2012).
[15]E. Hecht, *Optics*, 4th ed. (Addison-Wesley, Reading, MA, 2001).
[16]"For help with morphological filtering using MATLAB," see <http://www.mathworks.com/help/images/morphological-filtering.html>.
[17]The ImageJ homepage can be found at <http://rsbweb.nih.gov/ij/>.